

## Comparative Study of Flow in a Mixing Vessel Stirred by a Solid Disk and a Four Bladed Impeller

L. Mununga, K. Hourigan and M. Thompson

Fluids Laboratory For Aeronautical & Industrial Research (FLAIR)  
Department of Mechanical Engineering  
Monash University, Clayton Campus, Melbourne, Victoria 3800, Australia

### Abstract

Laminar flow in an unbaffled mixing vessel stirred by a solid disk rotor and a 4-blade impeller was simulated using the CFD software package FLUENT. The computational geometries and grids were generated using a pre-processor software package (Gambit) and then exported to Fluent where the rotating reference frame approach was employed to predict the flow field. The flow field is characterised by two recirculation regions, the centre of which was investigated. The swirl velocity and the Z-vorticity at the recirculation centre are much higher for the 4-blade impeller than for the solid disk rotor. Simulated results also show that both the swirl velocity and the Z-vorticity are higher near the impeller. Results show that at Reynolds number ( $Re$ ) = 200 the 4-blade impeller exhibits a sharp increase in the swirl velocity near the axis at the bottom of the mixing vessel, which generates an upwards vortical flow. The results show that the solid disk rotor may be viable for smooth laminar applications.

### Introduction

Mixing vessels find extensive industrial applications particularly in chemical, food and mining industries. The flow in mixing vessels is agitated by a single rotor or multiple rotors rotating within the fluid in the vessel. Rotors can be of different shapes depending on the objective of the mixing operation but they are broadly grouped as either radial flow [5] or axial flow [2]. Industrial mixing involves both single phase and multiphase systems.

The rotor, also known as the impeller, is a very important element of any mixing system. It provides the flow head and shear characteristics in accordance with the requirements of the process or operation [14]. As the rotor agitates the flow, recirculation regions form. Lamberto et al. [13] showed that the flow field in the tank generated by flat bladed turbines is divided in half and creates two distinct toroidal regions above and below the impeller. They also noted that the two regions acted as a barrier to mixing by increasing the blend time.

Process industry increasingly needs properly designed mixing vessels to reduce production losses and maintenance costs. The efficiency of many industrial processes greatly depends on the optimisation of the mixing parameters. It is therefore important to investigate flow generated in mixing tanks and be able to design systems with improved efficiencies. Bakker et al. [3] studied the effects of flow pattern on the solids distribution in a stirred tank and found that the solids distribution was strongly affected by certain flow transitions. As an alternative to experimental investigation, Computational Fluid Dynamics (CFD) constitutes not only a useful tool but also a cost effective means in the design of mixing systems.

Research work carried out in the past has looked at various aspects of mixing in stirred tanks and can be categorised as follows: in terms of the tank geometry the mixing tanks have been classified as baffled [4,15] or unbaffled [1,6], whereas in terms of flow regime mixing has been categorised as laminar [12] or turbulent [8,11].

Turbulent mixing vessel flow conditions closer to most real industrial applications have been investigated by previous workers [5]. The general perception that efficient mixing is achieved with turbulent mixing does not hold true for all applications. There are several applications for which turbulent mixing would be detrimental. For instance when the fluid is too viscous or contains substances that are shear sensitive, turbulent agitation may lead to unfavourable mixing conditions, hence laminar flow regime will be preferred. This research has been motivated by the fact that in some applications, as described above, a solid disk rotor would be more relevant than a bladed impeller. Bladed impellers represent too rapid a change of geometry in the flow, which leads to turbulence and higher shear rates. A solid disk rotor is thought to have the ability of producing a smoother mixing laminar flow at much higher Reynolds numbers ( $Re$ ) compared to a bladed impeller.

The work described here is part of a longer-term study to establish the effectiveness of solid disk rotors as an alternative to conventional agitators. This paper reports on preliminary study of the behaviour of the recirculation region in relation to the variation of  $Re$ . The study was limited to laminar flow spanning  $Re$  of 20, 50, 75, 100, 150 and 200. It is thought that the quality of the recirculation within the vessel affects the efficiency of mixing, but this will be examined in more detail in later studies.

### Numerical Model

The CFD package used to predict the velocity flow field was FLUENT version 5.5.14. Simulations were carried out for laminar flow regimes corresponding to  $Re$ : 20, 50, 75, 100, 150 and 200. The  $Re$  used in this study was based on the rotor diameter as shown in equation (1).

$$Re = (\rho ND^2) / \mu \quad (1)$$

where  $\rho$  is the fluid density ( $\text{kg/m}^3$ ),  $\mu$  is the fluid dynamic viscosity ( $\text{kg/ms}$ ),  $D$  is the rotor diameter (m) and  $N$  is the rotational speed of the rotor (rps).

The mixing vessel (Fig. 1) was 5.0 m high ( $H$ ) and 5.0 m in diameter ( $T$ ) and the rotor was placed mid-way along the vertical axis of the vessel. Two rotor geometries were used in the study. The first model made use of a solid disk of 1.0 m radius ( $r=D/2$ ) and 0.2r width ( $W$ , axial direction), whereas the second model employed a 4-blade radial flow impeller also known as a "Flat blade" impeller [14]. The tip radius of the blades,  $r$ , was 1.0 m while the blade width (axial direction) was 0.4r and the blade thickness (circumferential direction) was 0.1r. In Fig. 1 "C" is the distance from the rotor to the bottom of the tank also referred to as clearance.

The simulation fluid used in this work had a density of  $1.0 \text{ kg/m}^3$  and a dynamic viscosity of  $0.1 \text{ kg/ms}$ . The flow was assumed to be incompressible and steady. The following boundary conditions were used:

(i) **Solid disk:** A No-slip wall boundary condition was assumed at the vessel cylindrical wall, top lid and bottom. A rotating wall

boundary condition was assigned to the disk, which was modelled without a shaft (Fig. 2(a)).

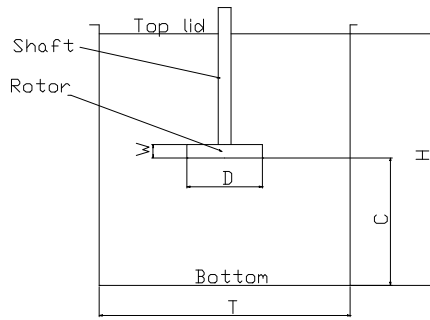


Figure 1. Typical mixing vessel with a rotor and a shaft.

(ii) **4-blade impeller:** The shaft and the impeller were stationary walls, in relative velocity formulation of the Rotating Reference Frame [7].

Gelfgat et al. [9] found that confined axisymmetric swirling flow in a closed circular cylinder with a rotating lid was still stable up to  $Re=2000$ . In a related study, Hourigan et al. [10] concluded that the apparent non-axisymmetry of the flow observed by other researchers was deceptive. Based on the above findings, the flow generated by the solid disk rotor was assumed to be symmetrical in the azimuthal direction and as a result only a  $30^\circ$  sector was modelled. The 4-blade impeller was modelled using a  $90^\circ$  sector. Both the geometries and grids were generated using a commercial software package called GAMBIT. The original grids were made of 7,500 hexahedral cells (50, axial direction, 25, radial direction, and 6, azimuthal direction) for the solid disk model and 61,250 hexahedral cells (70, axial direction, 35, radial direction, and 25, azimuthal direction) for the other model. The two grids were progressively adapted based on the pressure gradient and the resulting final grids had 97,283 cells for the solid disk model and 215,391 cells for the 4-blade model.

To simplify the mathematical simulation of flow in unbaffled vessels, as noted by Armenante et al. [1], the tank was filled with the experimental liquid up to the tightly fitted top lid cover, so as to prevent air from entering the system. The solid disk model was simulated in the Laboratory Frame of Reference (that is the frame of reference was attached to the tank wall) whereas the 4-blade model was simulated using the Rotating Reference Frame. In the Rotating Reference Frame, the impeller and the shaft are considered to be stationary relative to the frame of reference, while the outer wall (cylindrical tank wall), the bottom and top lid are given an angular velocity equal and opposite to that of the rotating frame. The above consideration results in constant boundary conditions and a time-independent velocity field. By employing the Rotating Reference Frame Fluent 5 offers a choice between using either the absolute velocity or the relative velocity formulation. Two velocities are to be considered: absolute velocity,  $V$ , and relative velocity,  $V_r$ , and they are related by the following equation:

$$V_r = V - \Omega \times r \quad (2)$$

where  $\Omega$  is the angular velocity of the rotating frame and  $r$  is the position vector in the rotating frame.

For the 4-blade impeller model, the segregated solver was utilised with the implicit formulation and the relative velocity formulation. The following discretization schemes were employed in the solution process: second-order for pressure,

second-order upwind for the momentum equation and SIMPLER for the pressure-velocity coupling.

## Results and Discussion

Results presented in this section were obtained from simulations performed for a mixing vessel agitated by a solid disk and a 4-blade impeller. Relevant results from the two models are presented on the same graph for ease of comparison. Since the rotor is centrally located within the tank most results are shown for the bottom half (right hand side in Fig. 2) of the viewing plane (vertical cross section through the tank). The viewing plane is located at  $45^\circ$  in the middle of the  $90^\circ$  grid sector between the blades (azimuthal direction). All post processing was performed in the laboratory reference frame. The results represent simulations for laminar flow corresponding to  $Re = 20, 50, 75, 100, 150$  and  $200$ .

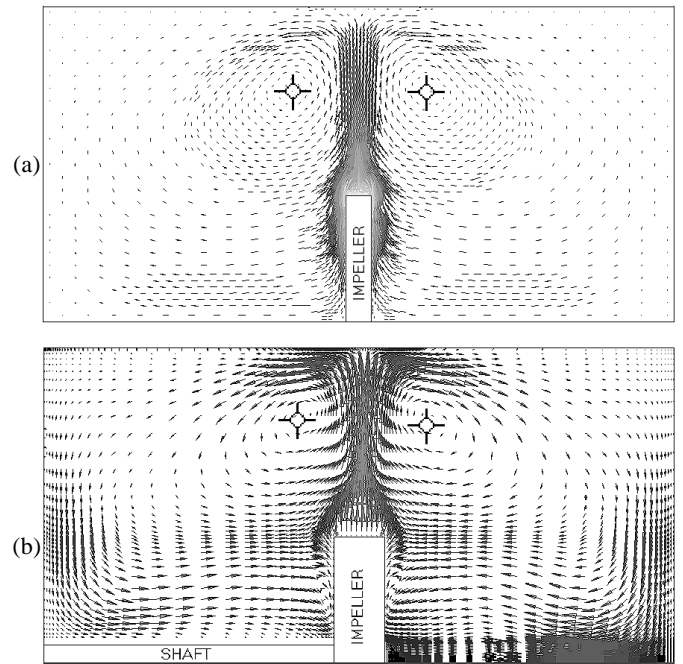


Figure 2. CFD prediction of axial and radial velocity components for  $Re=200$ : (a) solid disk model (with no shaft) (b) 4-blade impeller model.

Figs. 2 (a) & 2 (b) represent half view of the vessel vertical cross-section with the axial and radial components of the velocity vectors: (a) for the solid disk, and (b) the 4-blade impeller. In the above figures the vertical left and right sides correspond to the top lid and the bottom of the vessel respectively. The flow field is distinctly divided in two recirculation regions. The above flow field has been shown to occur in vessels agitated by radial flow impellers [12]. From the above observation the solid disk rotor can be classified as a “quasi-radial” flow impeller.

An important feature that is noticeable from the flow field of Fig. 2 is the centre of recirculation. This is focal point of the 2D flow shown in the figures where both the axial and radial velocity components are zero. However, the swirl or tangential component of velocity is non-zero, as shown in Fig. 5. The location of the centre of recirculation is shown in Fig. 3 for both the solid disk and the 4-blade impeller models. The recirculation centre is always further away, in the axial direction, from the solid disk compared to its position for the 4-blade impeller for the same  $Re$ . In both cases the location of the recirculation centre initially ( $Re=20$ ) tends to move towards the rotor. As  $Re$  increases beyond a critical region,  $75 < Re < 100$ , the centre of

recirculation tends to drift away from the rotor. It is thought that this observed change of direction will be largely dependent on both the  $Re$  and the radial dimension of the vessel.

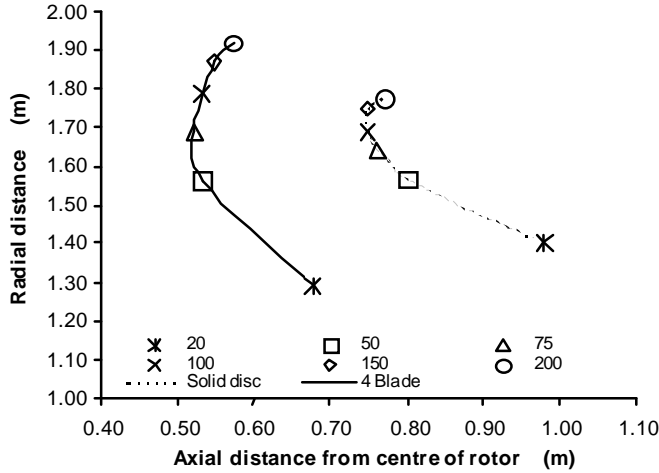


Figure 3. Location of the recirculation centre relative to the position of rotor (bottom half).

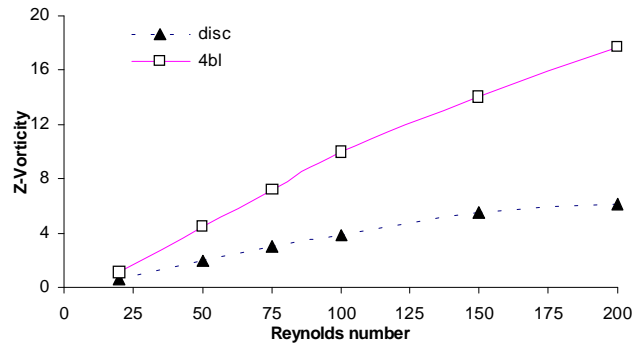


Figure 4. Variation of Z-Vorticity with  $Re$  at the recirculation centre.

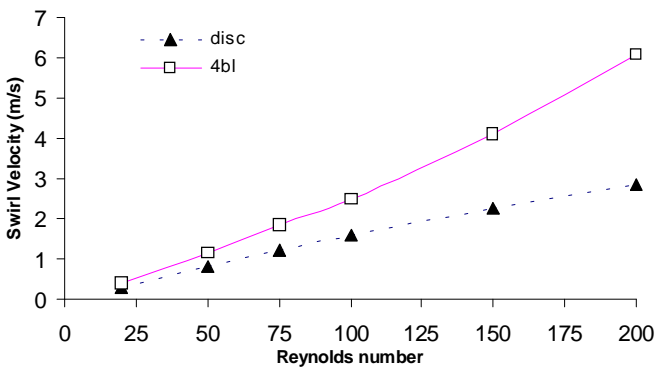


Figure 5. Variation of the swirl with  $Re$  at the recirculation centre.

Figs. 4 and 5 illustrate the variation of the Z-vorticity (azimuthal direction) and the swirl component of velocity, respectively, at the recirculation centre with respect to the  $Re$ . Fig. 5 demonstrates that the 4-blade impeller produces larger swirl velocities of about twice the magnitude of that produced by the solid disk. Similarly, the Z-vorticity generated by the 4-blade impeller is about 150% more than what is produced by the solid disk (Fig.4). The above results are not surprising because the 4-blade impeller has more contact surface with the fluid in the azimuthal direction than the solid disk has. However, the maximum vorticity for the 4-blade impeller model is only

marginally higher than it is for the solid disk model, as shown in Fig. 6. Other results, not included here, revealed that the maximum vorticity occurred in a localised zone near the tip of the rotors, where trailing vortices are found, for both cases.

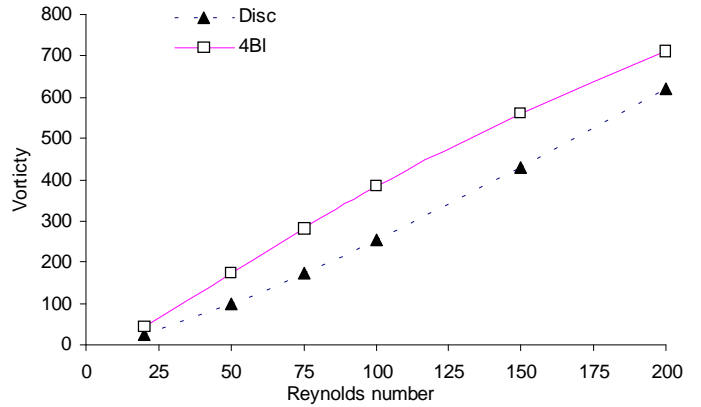


Figure 6. Variation of Maximum Vorticity with  $Re$ .

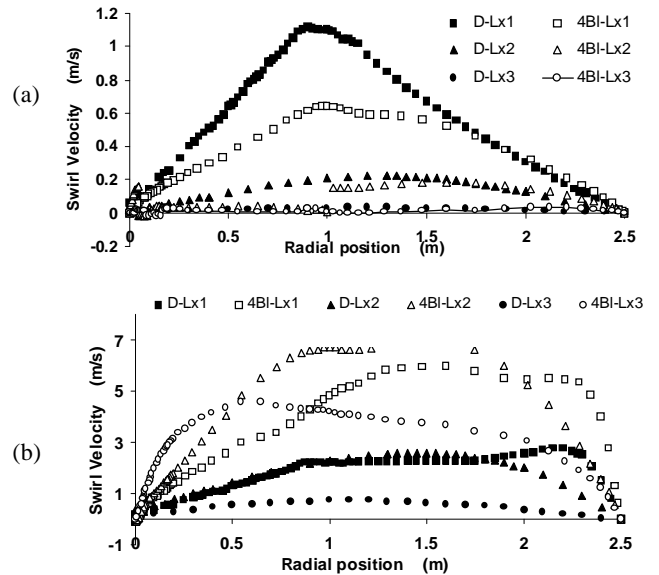


Figure 7. Swirl velocity profiles along three horizontal lines, Lx1, Lx2 and Lx3 (0.2m, 1.25m and 2.3m from the rotor respectively): (a)  $Re=20$  and (b)  $Re=200$ .

Figs. 7 and 8 display the variation of the swirl velocity and Z-vorticity along three horizontal lines, on the viewing plane, parallel to the bottom of the vessel for the two models (“D” and “4Bl” represent the solid disk and the 4-blade impeller models respectively). The three lines, Lx1, Lx2 and Lx3 are 0.2 m, 1.25 m and 2.3 m away from the rotor axis towards the bottom respectively. Fig. 7 (a) shows the swirl velocity at  $Re=20$  and as expected the velocity is highest near the rotor and almost zero near the bottom for both cases. Fig. 7 (b), at  $Re=200$ , reveals the same trend as in Fig. 7 (a) and in addition the swirl velocity along Lx3, near the bottom, and close to the axis of rotation is higher than along both Lx1 and Lx2. This result explains the existence of a vortical or “tornado” flow emanating from the bottom near the tank axis, which is characteristic of flow in unbaffled tanks. In Figs. 8 (a),  $Re=20$ , and (b),  $Re=200$ , the Z-vorticity distribution along the three horizontal lines shows that vorticity is higher closer to the rotor tip, i.e. at radii close to 1.0 m, where the maximum appears. However, vorticity tends to increase again

near the tank wall, due to the presence of the boundary layer, as clearly shown in Fig. 8 (b).

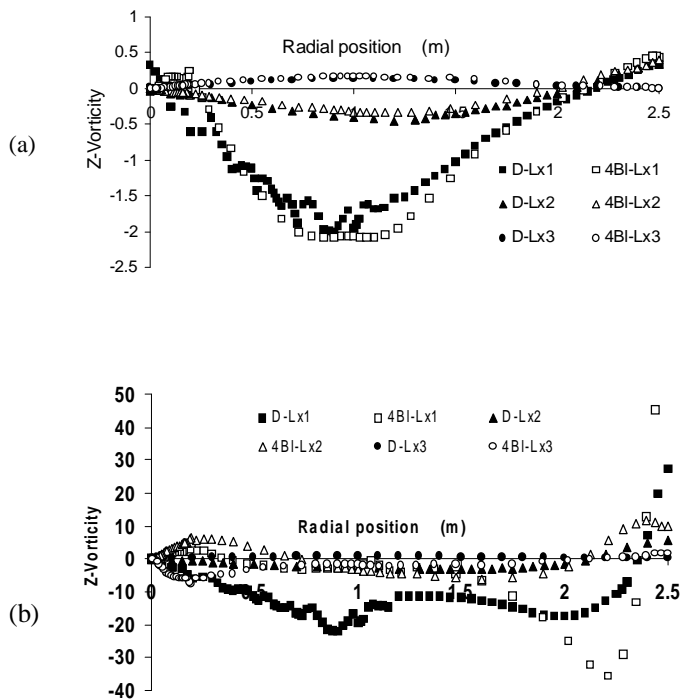


Figure 8. Z-vorticity profiles along three horizontal lines, Lx1, Lx2 and Lx3 (0.2m, 1.25m and 2.3m from the rotor respectively): (a)  $Re=20$  and (b)  $Re=200$ .

## Conclusions

A comparative study of laminar flow in an unbaffled mixing vessel agitated by a solid disk rotor and a 4-blade impeller has been carried out using CFD simulations. Computational results have revealed that the solid disk rotor produces a flow field similar to the one generated by the radial flow 4-blade impeller. The solid disk can be classified as a quasi-radial flow rotor. The location of the recirculation centre is seen to be further away from the solid disk rotor than it is from the 4-blade impeller for the same  $Re$ . In both cases the recirculation centre started moving towards the rotor as the  $Re$  was increased and between  $75 < Re < 100$ , which is a critical region, it drifted away. This phenomenon is worth further investigation with laminar and turbulent flow regimes. The swirl velocity and the Z-vorticity at the recirculation centre are much higher for the 4-blade impeller than they are for the solid disk rotor. The results show that the solid disk rotor may be viable for smooth laminar applications.

Simulation results also show that both the swirl velocity and the Z-vorticity are higher near the impeller. At  $Re=200$  the 4-blade impeller shows evidence of the development of a strong core flow near the rotational axis emanating from the bottom as a result of a sudden increase in the swirl velocity. The above phenomenon can be further investigated for both laminar and turbulent flow regimes.

Further similar studies will be carried out focusing on other aspects such as flow shear stress, input energy, and mixing efficiency to establish the field of application of the solid disk rotor.

## References

- [1] Armenante, P.M., Chou, C.C., Chun-Chiao, F. & Jaroslav, M., Velocity Profiles in a Closed, Unbaffled Vessel: Comparison Between Experimental LDV Data and Numerical CFD Predictions, *Chem. Engng. Sci.*, **52**, n20, October 1997, 3483-3492.
- [2] Armenate, P.M., Chou C.C. & Hamrajani, R.R., Comparison of Experimental and Numerical Fluid Velocity Distribution Profiles in an Unbaffled Mixing Vessel Provided with a Pitched-Blade Turbine, *Proceedings of the 8<sup>th</sup> European Conference on Mixing (IchemE Symp. Ser. No. 136)*, Cambridge, U.K., 21-23 Sept. 1994, 349-356.
- [3] Bakker, A., Fasano, J.B. & Myers, K.J., Effects of Flow Pattern on the Solids Distribution in a Stirred Tank, *Proceedings of the 8<sup>th</sup> European Conference on Mixing (IchemE Symp. Ser. No. 136)*, Cambridge, U.K., 21-23 Sept. 1994, 1-8.
- [4] Brucato, A., Ciofalo, M., Grisafi, F. & Micale, G., Complete Numerical Simulation of Flow Fields in Baffled Stirred Vessels: The Inner-Outer Approach, *Proceedings of the 8<sup>th</sup> European Conference on Mixing (IchemE Symp. Ser. No. 136)*, Cambridge, U.K., 21-23 Sept. 1994, 155-162.
- [5] Ciofalo, M., Brucato, A., Grisafi, F. & Torraca, N., Turbulent Flow in Closed and Free-Surface Unbaffled Tanks Stirred by Radial Impellers, *Chem. Engng. Sci.*, **51**, n14, July 1996, 3557-3573.
- [6] Dong, L., Johansen, S.T. & Eugh, T.A., Flow Induced by an Impeller in an Unbaffled Tank - I Experimental], *Chem. Engng. Sci.*, **49**, n4, Feb. 1994, 549-560.
- [7] Fluent Inc., FLUENT 5 User's Guide, Release 5.5, Lebanon, N.H., 1999.
- [8] Geisler, R., Krebs, R. & Forshuer, P., Local Turbulent Shear Stress in Stirred Vessels and Its Significance for Different Mixing Tasks, *Proceedings of the 8<sup>th</sup> European Conference on Mixing (IchemE Symp. Ser. No. 136)*, Cambridge, U.K., 21-23 Sept. 1994, 243-250.
- [9] Gelfgat, A. Yu, Bar-Yoseph, P.Z & Solan A., Stability of Confined Swirling Flow with and without Vortex Breakdown, *J. Fluid Mech.* **311**, 1996, 1-36.
- [10] Hourigan, K., Graham, L.J.W. & Thompson, M.C., Spiral Streaklines in Pre-vortex Breakdown Regions of Axisymmetric Swirling Flows, *Phys. Fluids* **7**, 1995, 3126-3128
- [11] Komori, S. & Murakami, Y., Turbulent Mixing in an Unbaffled Stirred Tank with Double Impellers, *6<sup>th</sup> European Conference on Mixing*, Pravia, Italy, 24-26 May 1988, 63-68.
- [12] Lamberto, D.J., Alvarez, M.M. & Muzzio, F.J., Experimental and Computational Investigation of the Laminar Flow Structure in a Stirred Tank, *Chem. Engng. Sci.*, **54**, 1999, 919-942.
- [13] Lamberto, D.J., Muzzio, F.J., Swanson, P.D. & Tonkovich, A.L., Using Time-Dependent RPM to Enhance Mixing in Stirred Vessels, *Chem. Engng. Sci.*, **51**, 1996, 733-741.
- [14] Oldshue, J.Y., Industrial Mixing Equipment, in *Encyclopaedia of Fluid Mechanics*, vol.2, Dynamics of Single-Fluid Flows and Mixing, Gulf Publishing Company, Houston, Texas, 1986, chap. 29.
- [15] Wong, C.W. & Huang, C.T., Flow Characteristics and Mechanical Efficiency in Baffled Stirred Tanks with Turbine Impellers, *6<sup>th</sup> European Conference on Mixing*, Pravia, Italy, 24-26 May 1988, 29-34.